Proceedings of the 7th International Symposium on Cavitation
CAV2009 – Paper No. 86
August 17-22, 2009, Ann Arbor, Michigan, USA

DRAG REDUCTION FOR HIGH-SPEED UNDERWATER VEHICLES

Igor Nesteruk
Institute of Hydromechanics, National Academy of Sciences of Ukraine
Kyiv, Ukraine

ABSTRACT

The very important problem of the underwater hulls drag reduction was investigated analytically and numerically with the use of the axisymmetric flow of the ideal and the viscous fluid approaches. Different effectiveness criteria, such as: the volumetric drag coefficient, the drag coefficients, based on the maximum body cross-section area and the squared hull length, and the ranges of the inertial motion were applied.

With the use of known analytic dependences for the slender axisymmetric cavity shapes after the slender or the non-slender cavitators, it was shown that the value of the volumetric drag coefficient and the similar coefficients, based on the squared values of the length and the caliber, can sufficiently be reduced at cavitation number less than 0.01. The smallest values of these drag coefficients correspond to the largest aspect ratios and the slender cavitators. Comparison of the drags of the supercavitating and unseparated flow patterns showed the existence of the critical values of the volume and sizes. The supercavitating flow pattern is preferable for the values of these parameters smaller than critical ones. For the horizontal supercavitation motion, the necessity of the Archimedes force compensation sufficiently diminishes the critical values of the vehicle volume or its sizes, which achieve maximum at a certain value of the motion velocity. In the case of the base cavity existence, the estimations of the supercavitating hull pressure drag and the comparison with the unseparated flow pattern are presented. The critical values of the body volume have a maximum at a certain value of the movement velocity and drastically increase with the aspect ratio increasing.

Maximum range problems are considered for the supercavitating motion of the axisymmetric body on inertia under an arbitrary angle to horizon in the case of very high velocities and non-slender cavitators. Different isoperimetric problems were formulated and solved with the fixed values of the body mass, kinetic energy, aspect ratio and caliber. Two dimensionless parameters are proposed which influence the solution. At small values of these parameters the optimal body shapes may use the nose part of the cavity only. Analytic and numeric solutions for the maximal range and the optimal body shapes are obtained. It was shown that infinite small exceeding of some critical value of the initial depth can cause a jump of the range and coming to the water surface. The corresponding values of the critical initial depth are calculated.

INTRODUCTION

The very important problem of the drag reduction of the high-speed underwater hulls can be solved with the use of different flow patterns. Some axisymmetric examples are shown in Figs. 1 and 2.

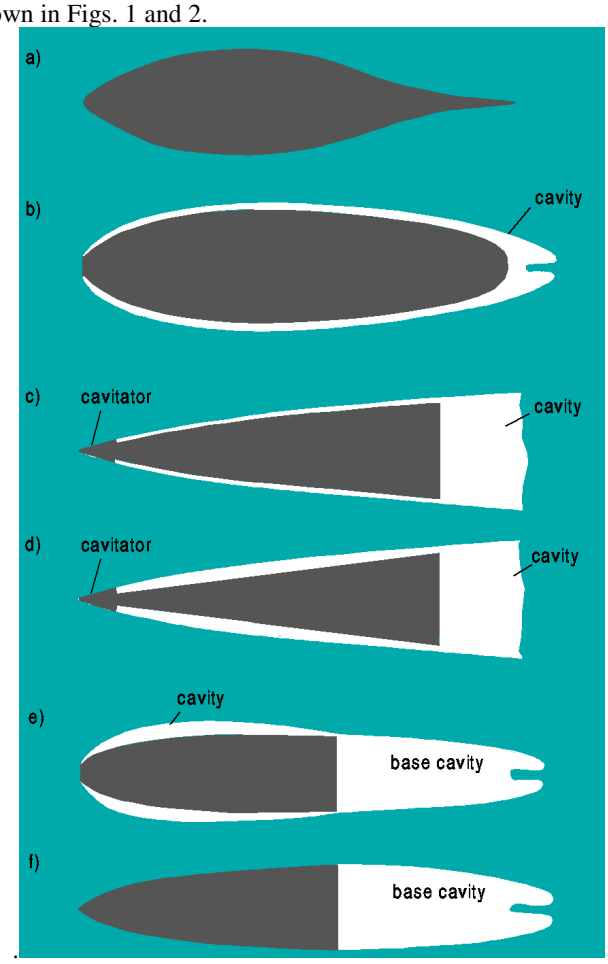

Figure 1: Different axisymmetric flow patterns.

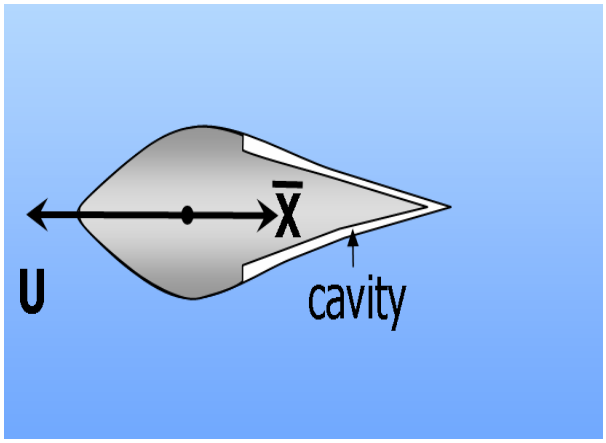

Figure 2: Non-standard cavitator and cavity which needs no closing body

The patterns, shown in Figs. 1a and 1f correspond to the flow without boundary layer separation and low pressure drag. The supercavitating flow patterns, shown in Figs. 1b, 1c, 1d, 1e, ensure low skin-friction drag due to the small surface of the cavitator wetted by water, but the pressure drag can be rather high. To create a cavity, the slender (Figs. 1c and 1d) and non-slender slender (Figs. 1b and 1e) cavitators can be used. The non-standard flow pattern with a cavity which closes without any artificial closing body or re-entrant jet (shown in Fig.2, see also [2]) could provide minimal pressure drag (due to the Dalambert paradox) and the skin-friction drag is reduced in comparison with the unseparated flow pattern shown in Fig. 1a (due to the smaller area wetter by water).

To compare the effectiveness of the different flow patterns different criteria can be used. If the vehicle velocity U_∞ and the hull volume V_b are fixed the simplest and effective criterion is the volumetric drag coefficient:

$$C_V \equiv \frac{2X}{\rho U_\infty^2 (V_b)^{2/3}} \qquad (1)$$

When the hull caliber D_b or its length L_b are fixed, the coefficients C_D or C_L can be used:

$$C_D \equiv \frac{8X}{\rho U_\infty^2 \pi D_b^2}, \qquad C_L \equiv \frac{2X}{\rho U_\infty^2 L_b^2} \qquad (2)$$

The estimations of C_V for the axisymmetric slender body without the boundary layer separation are presented in [1, 2]. For the pure turbulent boundary layer the following formula was obtained

$$C_{VU} \approx \frac{0.062}{\lambda_b^{10/21}\,\mathrm{Re}_V^{1/7}}, \quad \mathrm{Re}_V = \frac{U_\infty V_b^{1/3}}{\nu}, \quad \lambda_b = \frac{L_b}{D_b} \qquad (3)$$

The C_V estimations for the supercavitating hull which use the total cavity volume (Fig. 1b) can be found in [2] both for slender and non-slender cavitators. In particular, in [3] the following formula was obtained

$$C_V = \sqrt[3]{\frac{9\pi\sigma^4}{-16\ln\sigma}} \qquad (4)$$

for conic cavitators with the angle 2θ, $\theta > 25^0$. Equation (4) follows from the well known semi empiric formulas of Garbedian [4]

$$R^2 = \frac{x(1-x)}{\lambda^2}, \qquad \frac{R_n}{L} = \frac{\sigma}{2\sqrt{-C_x \ln\sigma}}, \qquad (5)$$

$$\lambda = \frac{L}{D} = \sqrt{\frac{-\ln\sigma}{\sigma}}, \qquad \frac{D}{R_n} = 2\sqrt{\frac{C_x}{\sigma}}$$

Here σ is the cavitation number σ; $R(x)$ is the cavity radius; R_n is the cavitator radius; λ is the cavity aspect ratio; D is the maximal cavity diameter; L is the cavity length; C_x is the cavitation drag coefficient related to the base section area of the cavitator πR_n^2. It must be noted that the value C_V does not depend on θ for these non-slender cavitators and tends to zero with diminishing of the cavitation number σ. The relationship (5) is represented in Fig. 3 by the dashed line. The results of non-linear numerical calculations for slender cones with the use of the method from paper [5] are presented by dots. The linear calculations with the use of formulas [6, 7]

$$\frac{R^2}{R_n^2} = \frac{\sigma x^2}{2R_n^2 \ln\beta} + 2\beta\frac{x}{R_n} + 1, \qquad (6)$$

$$C_x \approx C_{x0} = -2\beta^2\left[\ln(0.5\beta) + 1\right]$$

(β is the derivative of the radius at the point of cavity origin) are shown in Fig.3 by solid lines.

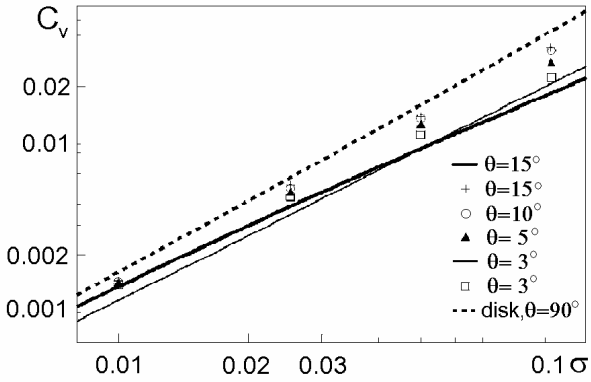

Fig. 3: Volumetric drag coefficients for cones.

Unfortunately, for the hull, which uses the total cavity volume (see Fig. 1b), the cavitation number cannot be diminished to zero, since the appropriate cavity aspect ratio λ tends to infinity (see, for example, (5)) when $\sigma \to 0$. The same value of λ_b has also the hull located in the cavity. The constructive considerations restrict the body aspect ratio. For example, if λ_b is limited by the value $\lambda_m = 20$, the possible cavitation numbers cannot be less than 0.01 for both the slender and the non-slender cavitators, and $C_V \geq 1.5 \cdot 10^{-3}$ (see Fig.3).

Formula (3) shows that $C_{VU} < 1.5 \cdot 10^{-3}$ for $\mathrm{Re}_V > 10^7$ and $\lambda_b = 20$. Thus, the standard supercavitating flow pattern (Fig. 1b) is preferable for smaller values of the volumetric Reynolds number $\mathrm{Re}_V < 10^7$ only. The cavitation number has to be close to minimal possible value $\sigma \approx 0.01$. The critical value of the volumetric Reynolds number can be increased for the hulls with the greater aspect ratio and corresponding less values of the cavitation number. For example, if $\lambda_b = 100$, the corresponding values of the cavitation number and C_V (according to the formulae (4),(5)) can be estimated as follows: $\sigma \approx 0.00072$, $C_V \approx 4 \cdot 10^{-5}$. It means that the drag is 37 times smaller in comparison with the case $\lambda_b = 20$. The supercavitating flow pattern is preferable for such slender hulls (in comparison with the unseparated one shown in Fig.1a) at all the values of the subsonic velocities and the vehicle dimensions of practical interest.

In the cases, when the aspect ratio increasing is impossible the only way of the supercavitation drag diminishing is to use the initial part of the cavity only (as shown in Figs. 1c and 1d). It looks confusing. Really, if the hull uses only a part of the cavity, then the volumetric drag coefficient increases (see formula (1)). But this fact enables us to use smaller cavitation numbers and larger cavities. As a result, the volumetric drag coefficient can be smaller for the flow patterns 1c and 1d in comparison with the 1b one. The detailed proof can be found in [8]. The main results for different values of the maximum hull aspect ratio λ_m are presented in Section 1.

The case of the flow patterns with the base cavity (see Figs. 1e and 1f) is also presented [8]. The principal results are reported in Section 2.

The maximum range problems are considered in [9] for the supercavitating motion of the axisymmetric body on inertia under an arbitrary angle to horizon in the case of very high velocities and non-slender cavitators. The vehicle can use the initial part of the cavity only. The main results are presented in Section 3 for different values of the maximum hull aspect ratio λ_m.

1. THE UNDERWATER HULLS DRAG DIMINISHING AT VERY HIGH SPEEDS

If the hull is located in the initial part of the cavity only (such as shown in Figs. 1c or 1d), the appropriate volumetric drag coefficients can be easily defined with the use of (1) and (5) for non-slender cavitator (or (6) in the case of the slender one). The analytical formulas can be found in [8], the calculation examples are presented in Fig. 4 for different values of the maximum hull aspect ratio λ_m. The lines correspond to the non-slender cavitators (the results do not depend on θ); the dots show the case of the slender cavitator with $\beta = 0.1$.

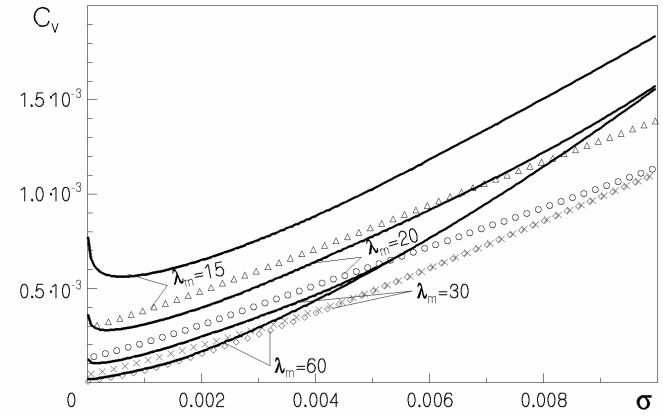

Fig. 4: Volumetric drag coefficients for different values of the hull aspect ratio.

It can be seen from Figs. 3 and 4 that C_V can be sufficiently reduced for $\sigma < 0.01$. The smallest values of C_V correspond to the largest values of the hull aspect ratio. In the case of the non-slender cavitators the function $C_V(\sigma)$ has a minimum. May be this fact is connected with the limited accuracy of the Garabedian formulae (5) for very small cavitation number in the region close to the cavitator. Usually, the slender cavitators yield smaller values of C_V. May be it is due to the limited accuracy of the equations (6). I any case this interesting fact needs additional investigations with the use of the second approximation equation [10] or a nonlinear approach.

An example of the optimal shape with $\lambda_m = 10$, $\beta = 0.1$, the velocity 700 m/s (the corresponding value of the cavitation number at small depth without ventilation is 0.0004, $L_b / R_n = 62.62$, $C_V = 0.00099$) is shown schematically in Fig. 1c. The optimal hull shape must be as close as possible the form of the initial part of the cavity. In the cases when the hull caliber or its length are fixed, the optimal hull must be only inscribed into the initial part of the cavity, but its caliber must coincide with the diameter of the cavity at the body end (see Fig. 1d). The dependences for coefficients C_D and C_L, which can be obtained with the use of formulae (2), (5) and (6), are

shown in Figs. 5 and 6 (see details in [8]). The lines correspond to the non-slender cavitators (the results do not depend on θ); the dots show the case of the slender cavitator with $\beta = 0.1$.

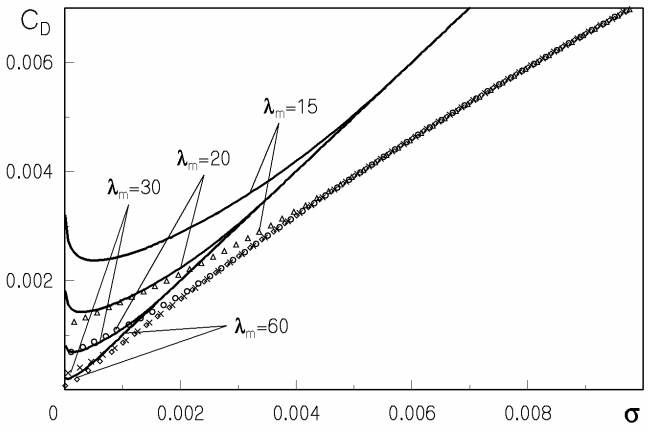

Fig 5: The drag coefficients C_D for different values of the hull aspect ratio.

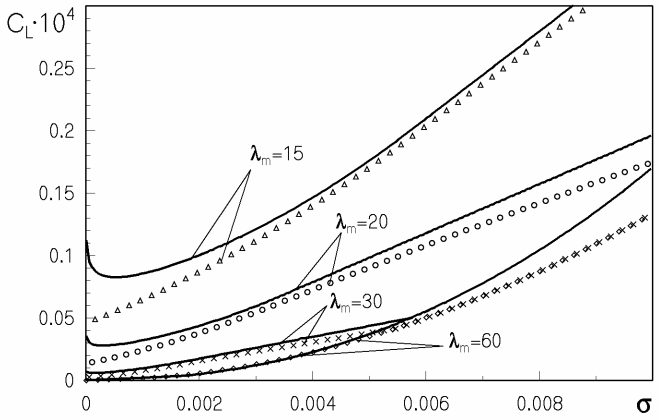

Fig 6: The drag coefficients C_L for different values of the hull aspect ratio.

The following equation

$$C_V = C_{VU} \qquad (7)$$

can be used to calculate the critical value of the volumetric Reynolds number Re_{V*} which corresponds to the equal efficiency of the unseparated (Fig.1a) and supercavitating (Fig. 1b, 1c and 1d) flow patterns. The supercavitating hull is preferable for $\mathrm{Re}_V < \mathrm{Re}_{V*}$. The drastic diminishing of C_V showed in Fig. 4 enables to increase the value of Re_{V*} at small cavitation numbers without increasing the hull aspect ratio.

For example, the optimal shape with $\lambda_m = 20$, the non-slender cavitator, the velocity 1000 m/s and a small depth of the horizontal movement (the corresponding value of the cavitation number is 0.0002, $C_V = 0.00028$) yields the critical values $\mathrm{Re}_{V*} \approx 1.2 \cdot 10^{12}$, $V^* \approx 10^9 m^3$. Therefore, the supercavitating flow pattern is preferable for all possible vehicles of practical interest.

On the other hand, the supercavitating hull moves in the gas (see Fig. 1b, 1c and 1d) with very small value of the Archimedes force in comparison with the wetted by water case shown in Fig.1a. Therefore, for supercavitating vehicles the problem of their weight compensation must be solved (as in the case of airplanes). For this purpose the hull planning on the cavity surface or underwater wings are used. This situation causes an additional drag with the coefficient ΔC_V, which can be estimated with the use of the aerodynamic effectiveness $k = C_y / C_x$. To calculate the critical Reynolds number, a new equation

$$C_V + \Delta C_V = C_{VU} \qquad (8)$$

should be solved instead of (7).

The numerical examples of solving equation (8) are presented in Figs. 7 and 8. The values $\nu = 1.3 \cdot 10^{-6} m^2 / s$, $k = 10$ (solid lines) and $k = 1$ (dots) were used for calculations.

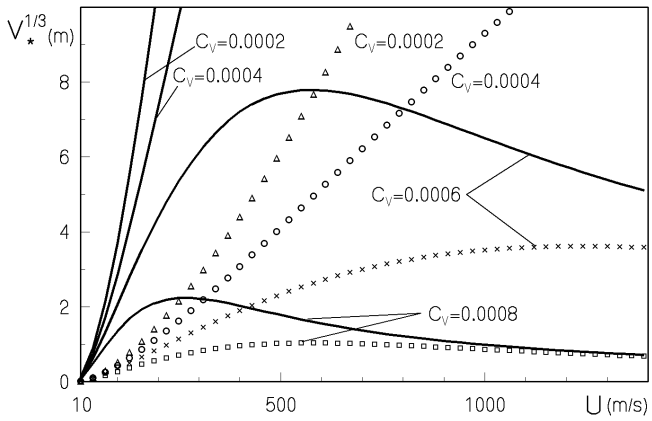

Fig 7: Dependences of the critical volume at different values of the volumetric drag coefficient C_V.

From Fig. 7 it can be seen that dependences have a maximum. The presented in [8] analysis enables obtaining the maximum values of the critical volume and the velocity corresponding to this maximum (see details in [8]). The critical volume decreases drastically with the increasing of C_V. Figs. 7 and 8 show also that the necessity of the Archimedes force compensation diminishes the critical volume (especially at small values of k and large values of C_V).The same

estimations of the critical hull calibre and its length can be done in the cases when these parameters are fixed (see details in [8]).

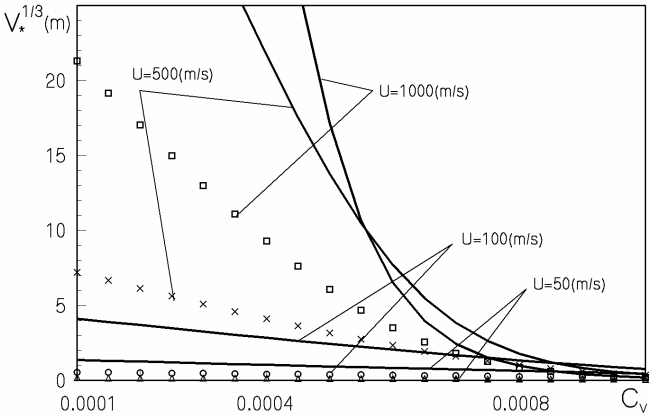

Fig 8: Dependences of the critical volume at different values of the velocity.

2. COMPARISON OF THE SUPERCAVITATING AND UNSEPARATED FLOW PATTERNS WITH THE BASE CAVITY

For the flows with the base cavity there are two options: 1) the hull is covered by another cavity (the two-cavity flow pattern shown in Fig. 1e); 2) the hull is wetted by the water flow without the boundary layer separation as shown in Fig. 1f. The comparison of efficiency of these two patterns was done in [8] with the use of formulae (6) for the pattern 1e and the parabolic unseparated shape

$$\frac{R}{R_n}=\frac{bx^2}{R_n^2}+1, \qquad -\sqrt{-\frac{1}{b}}\le\frac{x}{R_n}\le 0$$

for the flow pattern 1f.

Equation (8) was used to calculate the critical volume. The numerical examples are presented in Fig. 9. The values $\nu=1.3\cdot10^{-6}m^2/s$, $\beta=0.1$, $k=10$ (solid lines) and $k=1$ (dots) were used for calculations.

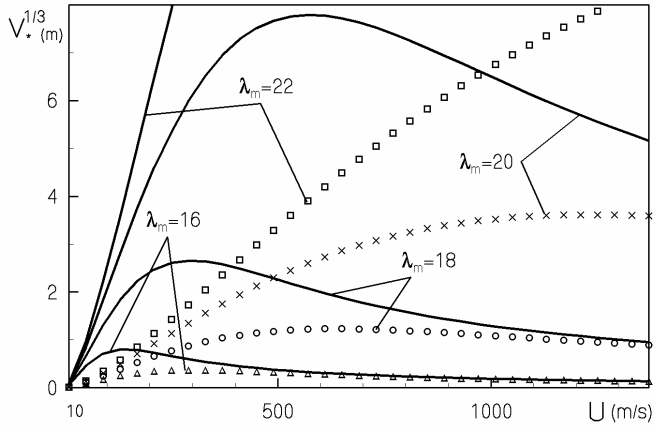

Fig 9: Dependences of the critical volume at different values of the hull aspect ratio for the base cavity flow pattern.

It can be seen from Fig. 9 that some curves have a maximum (similar as ones shown in Fig.7). The corresponding velocity increases with the hull aspect ratio increasing and may approach to the sonic velocity in water. The critical volume increases drastically with the increasing of the hull aspect ratio. Fig. 9 shows also that the necessity of the Archimedes force compensation diminishes the critical volume (especially at small values of k and large values of λ_m)

3. OPTIMIZATION PROBLEMS FOR HIGH-SPEED SUPERCAVITATION MOTION ON INERTIA

The results obtained in Section 1 stimulated the investigation of the effectiveness of the supercavitating flow pattern for the inertial motion with very small cavitation numbers. The horizontal supercavitating motion on inertia and the problem of range maximization were considered by Putilin, Gieseke, Serebriakov, Kirschner, Schnerr [15-18] and other authors. The case of the non-horizontal inertial motion with different isoperimetric conditions was investigated in [2, 11-14], but it was taken into account only the case of complete using the cavity volume (Fig. 1b). The case of partial cavity using (Fig. 1c and 1d) is typical for very small cavitation numbers and was investigated in [9] for non-slender cavitators. Here will be shortly reported the results of the paper [9].

Let the model start with the velocity U_0 under an arbitrary angle γ to horizon and then move in water on inertia. The distance S , passed by the supercavitating body, must be maximal (see Fig. 10). It was shown (see, for example, [12, and 13]) that in many cases the flow may be supposed as quasi-stationary and the gravity effect on the cavity and body motion may be neglected. If the cavitator is non-slender, the semi-empirical relations (5) by Garabedian may be used with the current cavitation number σ at the cavitator immersion depth. If we neglect changes of the cavitation number $\sigma<<1$, then C_x may be considered to be constant and the distance S passed by the body is defined by the following formula:

$$S=\frac{2m}{\rho C_x \pi R_n^2}\ln\frac{U_0}{U}, \qquad (9)$$

where m is the body mass; U is the final body velocity.

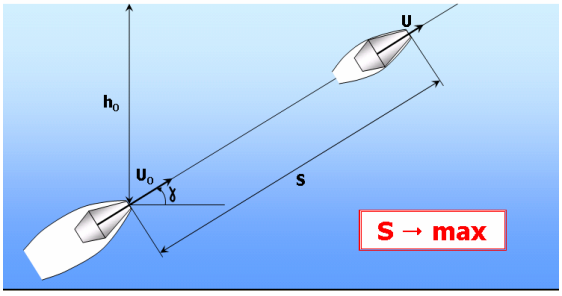

Fig. 10: The maximum range problem for the supercavitating motion on inertia

In [9] formula (9) is analyzed for different isoperimetric conditions. If the body mass, its caliber and aspect ratio are fixed, there is no need to investigate the case of the fixed body length. The volume of the hull located in the initial part of the cavity after a non-slender cavitator can be estimated as a cone volume (see Figs.1c and 1d); therefore there is no need to use the isoperimetric condition with the fixed volume. Thus, it is necessary to investigate the first problem only from the list, presented in [13, 14]:

1. The body mass and its caliber D_b are fixed;
2. The body mass and its length L_b are fixed;
3. The body mass and its volume V_b or the average body density $\rho_b = m/V_b$ and its volume are fixed;
4. The average body density and its caliber are fixed;
5. The average body density and its length are fixed.

Both the natural and the ventilation cavitation will be taken into account with the given value of the cavity pressure p_c at the final moment of the hull washing off and the vehicle stop. The cavitation number can be rewritten as follows:

$$\sigma = \frac{2gh_2}{U_0^2 \overline{U}^2}, \qquad \overline{U} = \frac{U}{U_0}, \qquad (10)$$

The final depth h and $h_2 = 10 + h - p_c$ are measured in meters.

3.1 PROBLEMS WITH THE FIXED FINAL DEPTH

If in addition to the body mass, caliber, aspect ratio, final depth its final velocity is also fixed, the final cavitation number will be also fixed (see (10)). Then the Garabedian formulae (5) allow calculating the hull shape and the cavitator diameter. Equation (9) shows that maximum range corresponds to the maximal starting velocity. The same trivial solution will be in the case of complete cavity volume using (Fig. 1b) and for all 5 problems listed above.

If instead of mass the initial body kinetic energy T_0 is fixed, then the optimal values of final velocity and body mass can be calculated (see details in [9])

$$\overline{U}^* = e^{-0.5} \approx 0.607, \qquad (11)$$

$$m^* = \frac{2T_0}{eU^2}.$$

The fixed initial velocity case is more difficult. But if the cavity volume is used completely (Fig. 1b), the same relationship (11) was obtained in [11]. For other 4 listed isoperimetric condition, other relationships for the optimal velocities ratio were obtained in [11] with the use of the 1b pattern. The case of the partial using of the cavity volume (Fig. 1c and 1d) needs solving the non-linear equations and depends on the dimensionless parameter $\overline{H}$

$$\overline{H} = \frac{gh_2}{U_0^2}, \qquad \overline{S}^* = \frac{S^* D_b}{U_0}\sqrt{\frac{\rho g}{m}}.$$

The results for the dimensionless maximum range $\overline{S}^*$ (solid lines) and optimal final cavitation number σ^* (dashed lines) are presented in Fig. 11 for different values of the hull aspect ratio. The range increases with the increasing of the aspect ratio, but the differences are sufficient for the very small values of the parameter $\overline{H}$ only. For $\overline{H} > 0.001$ and $\lambda_m > 15$ the obtained solution is practically independent of $\overline{H}$ and coincide with the results for the flow pattern 1b reported in [11].

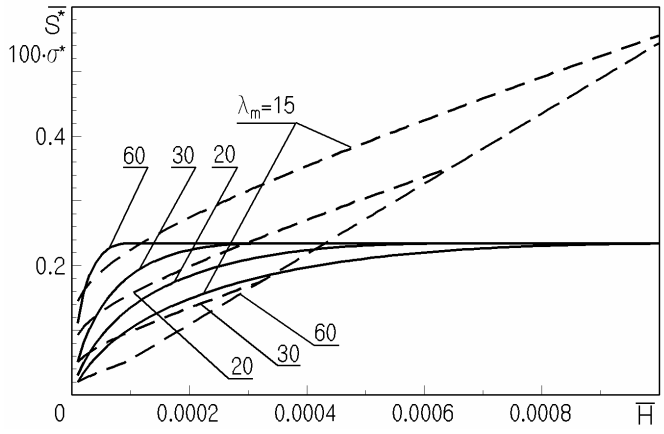

Fig 11: Dependences of the maximum range and optimal final cavitation number for different values of the hull aspect ratio.

The conclusion that the optimal hull caliber must coincide with the maximum final cavity diameter (see [11]) is no more valid for the case of very high velocities (small values of $\overline{H}$). To illustrate this fact, an example of optimal shape is shown in Fig. 12. The parameters of this supercavitating hull are $\lambda_m = 3, \overline{H} = 0.001$. The optimal range $\overline{S}^* \approx 0.083$ exceeds the ranges of any other hull with the same values of $\overline{H}$ and λ_m . For example, if the hull caliber coincides with the maximum final cavity diameter, then $\overline{S}^* \approx 0.063$ only.

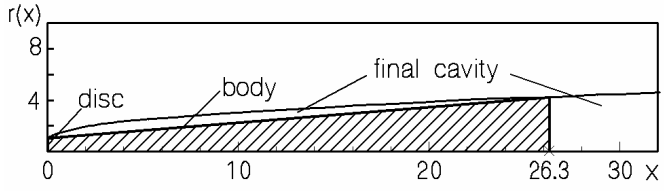

Fig 12: An example of the optimal body shape for $\lambda_m = 3$, $\overline{H} = 0.001$

3.2 PROBLEMS WITH THE FIXED INITIAL DEPTH

When the initial depth h_0 is fixed, the relation for h_2 can be rewritten as follows:

$$h_2 = h_1 - S\sin\gamma\,, \qquad h_1 = 10 + h_0 - p_c\,.$$

It means that the cavitation number and the solutions of the problem will depend on the angle γ (see 10). The nonlinear dependences make the search for the optimal solution more complicated.

If in addition to the body mass, caliber, aspect ratio, initial depth its final velocity is also fixed, the maximum range corresponds to the maximal starting velocity. The same trivial solution will exist in the case of complete cavity volume using (Fig. 1b) and for all 5 problems listed above.

If instead of final velocity the initial one is fixed, the solution is non trivial and depends on the dimensionless parameters $\overline{N}\,, \overline{h}_1$

$$\overline{N} = \frac{mg}{\rho U_0^2 D_b^2}\,, \qquad \overline{h}_1 = \frac{h_1 D_b}{U_0}\sqrt{\frac{\rho g}{m}}\,.$$

The results for the dimensionless maximum range $\overline{S}^*$ (solid lines) and optimal final cavitation number σ^* (dashed lines) are presented in Fig. 13-15 for different values of the hull aspect ratio. The range increases with the increasing of the aspect ratio, but the differences are sufficient for the very small values of the parameter $\overline{N}$ only. For $\overline{N} > 3\cdot 10^{-7}$ and $\lambda_m > 15$ the obtained solution is independent of $\overline{N}$ and coincide with the results for the flow pattern 1b obtained in [13].

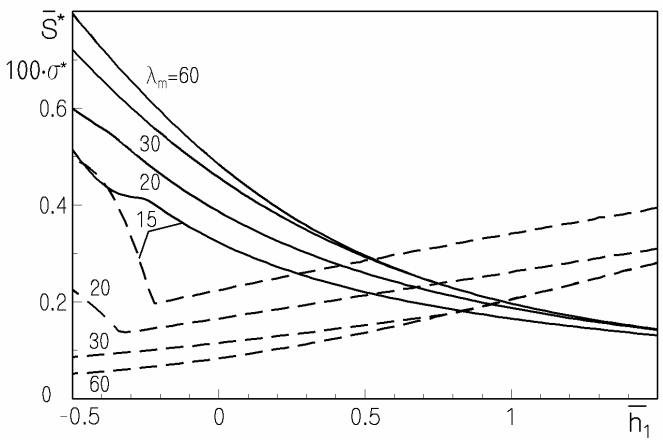

Fig 13: Dependences of the maximum range and optimal final cavitation number for different values of the hull aspect ratio at $\overline{N} = 10^{-7}$, $\gamma = -90^o$.

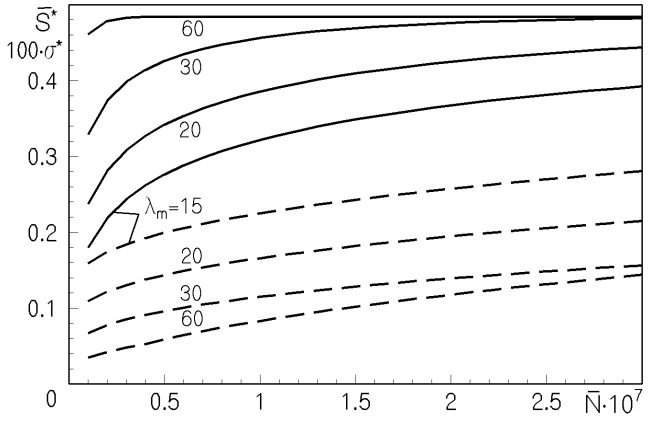

Fig 14: Dependences of the maximum range and optimal final cavitation number for different values of the hull aspect ratio at $h_1 = 0$, $\gamma = -90^o$.

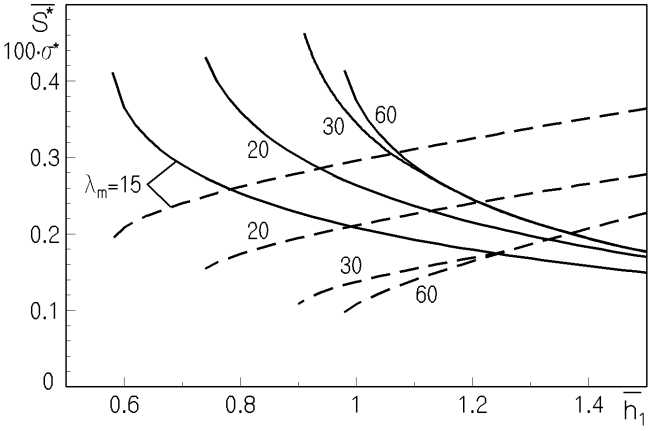

Fig 15: Dependences of the maximum range and optimal final cavitation number for different values of the hull aspect ratio at $\overline{N} = 10^{-7}$, $\gamma = 90^o$.

The numerical analysis showed that for $\gamma > 0$ the solution exist only for the values of $\overline{h}_1$ which are greater than the critical one $\overline{h}_1^{(cr)}$. The situation is similar to the flow pattern 1b investigated in [13]. It means that for smaller values of the initial depth the body can reach the free water surface without a loss of the supercavitating flow pattern. The critical values $\overline{h}_1^{(cr)}$ can be seen in Fig. 15. Increasing the hull aspect ratio increases $\overline{h}_1^{(cr)}$, which tends to the value

$$\overline{h}_1^{(cr)} = \sqrt{\frac{8\sin\gamma}{e\pi}}$$

obtained in [13l for the flow pattern 1b.

CONCLUSION

The value of the volumetric drag coefficient and the similar coefficients, based on the squared values of the length and the caliber, can sufficiently be reduced at cavitation number less than 0.01. The smallest values of these drag coefficients correspond to the largest aspect ratios and the slender cavitators. Comparison of the supercavitating and unseparated flow patterns showed the existence of the critical values of the volume and sizes. The supercavitating flow pattern is preferable for the values of these parameters smaller than critical ones. For the horizontal supercavitation motion, the necessity of the Archimedes force compensation sufficiently diminishes the critical values of the vehicle volume or its sizes, which achieve maximum at a certain value of the motion velocity. In the case of the base cavity, the comparison the supercavitating and the unseparated flow patterns is presented. The critical values of the body volume have a maximum at a certain value of the movement velocity and drastically increase with the aspect ratio increasing.

Maximum range problems are considered for the supercavitating motion of the axisymmetric body on inertia under an arbitrary angle to horizon. Different isoperimetric problems were formulated and solved with the fixed values of the body mass, kinetic energy, aspect ratio and caliber. Two dimensionless parameters are proposed which influence the solution. At small values of these parameters the optimal body shapes may use the nose part of the cavity only. Analytic and numeric solutions for the maximal range and the optimal body shapes are obtained. It was shown that infinite small exceeding of some critical value of the initial depth can cause a jump of the range and coming to the water surface.

ACKNOWLEDGMENTS

Author thanks Dr. M. Makasyeyev from National Technical University of Ukraine “Kyiv Polytechnic Institute” for interesting and useful discussions of the paper.

REFERENCES

[1] Nesteruk I., 2002, “The Problems of Drag Reduction in High Speed Hydrodynamics’, The International Summer Scientific School “High Speed Hydrodynamics”, June 16-23, 2002, Cheboksary, Russia.- P. 351- 359.

[2] Nesteruk I., 2006, “Drag reduction in high-speed hydrodynamics: supercavitation or unseparated shapes”, CAV2006.

[3] Nesteruk I., 2003, “Drag calculation of slender cones using of the second approximation for created by them cavities”, Prykladna gidromekhanika (Applied Hydromechanics), Kyiv, 5(77), No. 1. pp. 42-46. (in Ukrainian).

[4] Garabedian P.R., 1956, “Calculation of axially symmetric cavities and jets”, Pac. J. Math., Vol.6, No.4, pp. 611-684.

[5] Nesteruk I., 2003, ”Simulation of axisymmetric and plane free surfaces by means of sources and doublets”, Applied Hydromechanics, Kyiv, 5(77), No. 2: 37-44. (in Ukrainian)

[6] Nesteruk I., 1979, “Investigation of Slender Axisymmetric Cavity Form in Fluid with Gravity”, Izv. AN SSSR, MFG, No.6, pp.133-136 (in Russian)

[7] Nesteruk I., 1982, “Some Problems of Axisymmetric Cavity Flows“, Izv. AN SSSR, MFG, No. 1, pp. 28-34.(in Russian.).

[8] Nesteruk I, 2009, “Drag diminishing of long axisymmetric high-speed bodies”, Applied hydromechanics, Vol. 11 (83), No. 2, pp. 55 - 67 , (in Ukrainian).

[9] Z.I. Manova, I. Nesteruk, B.D. Shepetyuk, 2009, “Optimization problems for high-speed supercavitation motion on inertia with the non-slender cavitators”, Applied hydromechanics, Vol. 11 (83), No. 4, (to be published in Ukrainian).

[10] Nesteruk I., 1985, “The Slender Axisymmetric Cavity Form Calculations Based on the Integral-Differential Equation”, Izv. AN SSSR, MZhG, No.5, pp.83-90. (in Russian).

[11] Nesteruk I., Semenenko V.N., 2006, “Problems of optimization of range of the supercavitation inertial motion at the fixed final depth”, Applied hydromechanics, v.8, No 4, pp.33-42 (in Ukrainian).

[12] Nesteruk I., Savchenko Yu .M. Semenenko V.N., 2006, “Range optimization for supercavitating motion on inertia”, Reports of Ukrainian Academy of Sciences, N 8 , pp. 57-66. (in Ukrainian).

[13] Nesteruk I., 2008, ‘Range maximization for supercavitation inertial motion with the fixed initial depth”, Applied hydromechanics, Vol. 10 (82), No. 3, pp. 51 - 64 , (in Ukrainian).

[14] Nesteruk I., 2008, “Hull optimization for high-speed vehicles: supercavitating and unseparated shapes”, International Conference SuperFAST2008, July 2-4, 2008, Saint-Petersburg, Russia.

[15] Putilin S.I., 2000, “Some features of dynamics of supercavitating models”, Applied hydromechanics, Vol.2 (74), No.3, pp. 65-74. (In Russian).

[16] Gieseke T.J., 2001, “Toward an optimal weapon system utilizing supercavitating projectiles, Int. Conference on Cavitation "Cav2001", Pasadena, USA, Session B3.002.

[17] Serebryakov V.V., 2002, “The models of the supercavitation prediction for high speed motion in water”, Int. Summer Scientific School "High Speed Hydrodynamics". Cheboksary, Russia, pp. 71-92.

[18] Serebryakov V.V., Kirshner I.N., Scherr G.H., “Some problems of high speed motion in water with supercavitation for sub-, trans- and supersonic mach numbers”, Proceedings of the X International scientific school “High-speed hydrodynamics” and International conference «Hydromechanics. Mechanics. Power-plants» (to the 145-th anniversary of academician A.N.Krylov), Cheboksary department of Moscow State Open University, Moscow – Cheboksary, ISBN 978-5-902891-35-2, pp. 73-104.